Optics of multilayered conducting systems: Normal modes of periodic superlattices

W. Luis Mochán and Marcelo del Castillo-Mussot
Instituto de Física, Universidad Nacional Autónoma de México, Apartado Postal 20-364, 01000 México, Distrito Federal, Mexico
(Received 24 July 1987; revised manuscript received 11 December 1987)

We develop a 4×4 transfer-matrix formalism in order to study, within the hydrodynamic model of electron dynamics, the optics of multilayered conducting heterostructures, taking into account retardation and the coupling between transverse and longitudinal waves at the conductor boundaries. The dispersion relation of the electromagnetic normal modes of an infinite periodic superlattice is calculated in the retarded and the nonretarded regimes, yielding a very rich structure, as a consequence of several propagation mechanisms which are discussed in detail. The dependence of the results on the set of additional boundary conditions imposed at the surfaces is also examined.

I. INTRODUCTION

The electromagnetic normal modes of multilayered heterostructures have received considerable attention lately. Most of it has been directed towards semiconductor heterostructures, for which the charge carriers of one or more of its layers may constitute a quasi-two-dimensional electron or hole gas. The bulk modes arising from the coupling among the two-dimensional (2D) plasmons[1] of each 2D conductor have been investigated for periodic[2] superlattices, as well as the surface plasmons for truncated superlattices[3] and localization effects for aperiodic structures.[4,5] The effects of the possible excitation between a few size-quantized, low-lying electronic energy levels have also been considered.[6] Qualitatively different heterostructures are obtained by heavily doping the semiconductor layers[7] or by replacing them altogether with metallic ones.[8] Each conducting layer thus obtained can sustain collective modes such as surface and bulk plasmons, which yield a very rich structure for the normal modes of the composite system, whose study is the subject of this paper.

The bulk and surface modes of conductor-insulator and conductor-conductor infinite and semi-infinite periodic superlattices were first obtained using a local model for the conducting layers in the nonretarded,[9] and later in the retarded,[10] regimes. The effects of spatial dispersion were introduced later[11] within an effective-medium approximation[12] using a perturbative formulation.[13] In order to take into account the propagation of bulk plasmons within one or more of the layers, a hydrodynamic model has been solved disregarding retardation to obtain the dispersion relation[14] and the electron energy-loss spectra[15] for infinite superlattices. Very recently, the modes of a single conducting layer within an infinite conductor were also calculated within a hydrodynamic model including retardation effects.[16]

In some of the hydrodynamic calculations above, the fields within any one layer were expressed as a superposition of the fields produced by all the other layers in the system, leading to integro-differential equations which were solved taking advantage of the simple geometries chosen. The generalization of the methods of solution employed to other layered geometries does not seem immediate. In other calculations, the fields within each layer were expressed as a superposition of plane waves, and boundary conditions were imposed at each interface. The size of the system of equations thus obtained seems to grow with the number of different layers in the system.

On the other hand, the fields at an arbitrary position within a layered system are completely determined if enough field components are specified at any fixed reference position. Therefore, the propagation of waves through this kind of system is best studied by introducing the transfer matrix which relates the fields at different positions. Clearly, the transfer across several layers is accomplished simply by multiplying the transfer matrices corresponding to each of them. Transfer-matrix formalisms are used routinely in the design of optical filters[17] and for the interpretation of seismic data.[18] They have also been employed successfully in calculating the resistance of disordered conductors[19] and in predicting the existence of critical plasmons in quasiperiodic semiconductor superlattices.[5]

In a previous paper, we have developed a 2×2 transfer-matrix formalism for conductor-insulator superlattices.[20,21] The results were later generalized[22] to conductor-conductor superlattices by assuming that plasmons were confined within the low-density conductors. The purpose of this paper is the construction of an exact transfer-matrix formalism appropriate for conducting multilayered systems within hydrodynamic models, introducing no extra assumptions. Thus our formalism can be used in the retarded as well as in the nonretarded regimes, and it takes into account the propagation of plasma waves in each layer, their coupling to p-polarized transverse waves at each interface, and their transmission into adjacent layers. Other nonlocal effects may be incorporated later using perturbative approaches.[13] Since hydrodynamic models have usually been formulated for homogeneous systems and there is no accord yet over which are the nonelectromagnetic boundary conditions obeyed by the fields,[23-25] our results are written in a way which is independent of the boundary conditions, so that a comparison between the predictions of different models of conductor boundaries can be performed within the same formalism.

As a first application of our formalism, we obtain analytical expressions for the dispersion relation of the electromagnetic normal modes pertaining to an infinite periodic superlattice built from two alternating conductors. We also investigate the effects of retardation and of the choice of boundary conditions. A profusion of modes is obtained, several of which have not been reported before, and their composition is described in detail.

The paper is organized as follows: In Sec. II, we construct the transfer matrix for a single conducting layer, from which that of any heterostructure can be obtained by simple multiplication. We also obtain analytically the normal modes of the periodic superlattice. In Sec. III, we present and discuss the results of calculations for a highly doped semiconductor superlattice, and we devote Sec. IV to conclusions.

II. THEORY

In this section, we develop a transfer-matrix formalism which permits the calculation of the optical properties of multilayered conducting heterostructures within the hydrodynamic model. For concreteness, we consider the superlattice shown in Fig. 1 consisting of alternating layers of conductors a and b stacked along the Z direction. In order to obtain the transfer matrix of the system, we start by constructing the transfer matrix of one conducting layer, following a procedure similar to the one discussed in Ref. 20.

A. Transfer matrix of one layer

In a given layer there are two p-polarized waves moving towards the right and left with wave vectors $\mathbf{q}_{\pm}^{\mathrm{T}}=(Q,O,\pm q^{\mathrm{T}})$, such that

$$(q^{\mathrm{T}})^2=\epsilon^{\mathrm{T}}(\omega)\frac{\omega^2}{c^2}-Q^2 . \tag{1}$$

There are also two longitudinal waves with wave vectors $\mathbf{q}_{\pm}^{\mathrm{L}}=(Q,O,\pm q^{\mathrm{L}})$, obeying

$$\epsilon^{\mathrm{L}}(\mathbf{q}_{\pm}^{\mathrm{L}},\omega)=0 . \tag{2}$$

Here,

$$\epsilon^{\mathrm{T}}(\omega)=\epsilon^{\mathrm{B}}(\omega)-\frac{\omega_p^2}{\omega^2+i\omega/\tau} \tag{3}$$

is the local transverse dielectric function of the layer,

$$\epsilon^{\mathrm{L}}(\mathbf{q},\omega)=\epsilon^{\mathrm{B}}(\omega)-\frac{\omega_p^2}{\omega^2+i\omega/\tau-\beta^2\,|\,q\,|^{2}} \tag{4}$$

is its spatially dispersive longitudinal dielectric function, $\epsilon^{\mathrm{B}}(\omega)$ is the local contribution from the interband transitions to its dielectric response, ω_p is the plasma frequency of its conduction-electron gas, τ is a phenomenological damping constant, and β is its stiffness constant. Translational invariance along the X-Y plane and in time allows us to consider only waves with the same wave-vector projection unto the X-Y plane $(Q,0)$ and a given frequency ω. Most quantities above, such as q^{T}, ϵ^{T}, ϵ^{L}, etc., depend on which layer, a or b, is being considered; this dependence is implied throughout the present subsection in order to simplify our notation.

Since there are four waves in each layer for each ω and Q, the fields anywhere inside the layer can be determined from any four independent components at one point. It is convenient to choose components which are continuous at the layers' boundaries. Electromagnetic theory implies the continuity of E_x and B_y, the components of the electric and magnetic fields parallel to the surface.[26] The identity of the other two independent continuous field components cannot be determined from electromagnetic theory alone, and it is the object of the much-debated additional-boundary-condition (or ABC) controversy.[23–25] Different ABC's correspond to different assumptions about the microscopic response of the conductor near its surface.[27] However, we have found that several well-known ABC's can be expressed as the continuity of μj_z and of $4\pi i\nu\rho$, where j_z is the normal to the surface component of the conduction current density, ρ is the charge-density fluctuation induced in the electron gas, and μ and ν are constant parameters within each layer. We will refer to the choices $\mu=1$, $\nu=\beta^2/\omega_p^2$ as model I,[28] $\mu=1/\omega_p^2$, $\nu=\beta^2$ as model II,[29] and $\mu=1$, $\nu=1$ as model III.[30]

Having chosen the four independent field quantities $E_x(z)$, $B_y(z)$, $\mu j_z(z)$ and $4\pi i\nu\rho(z)$, we proceed to find how they are related at different points inside a layer. This is most simply done by writing them in terms of the right- and left-moving contributions to the magnetic field, $B_+(z)$ and $B_-(z)$, and to the scalar potentials $\phi_+(z)$ and $\phi_-(z)$ in the Coulomb gauge:

$$\begin{bmatrix} E_x \\ B_y \\ \mu j_z \\ 4\pi i\nu\rho \end{bmatrix}_z = \underline{G} \begin{bmatrix} B_+ \\ B_- \\ \phi_+ \\ \phi_- \end{bmatrix}_z , \tag{5}$$

where

$$\underline{G}=\begin{bmatrix} \dfrac{q^{\mathrm{T}}c}{\epsilon^{\mathrm{T}}\omega} & -\dfrac{q^{\mathrm{T}}c}{\epsilon^{\mathrm{T}}\omega} & -iQ & -iQ \\ 1 & 1 & 0 & 0 \\ -\mu\sigma^{\mathrm{T}}\dfrac{Qc}{\epsilon^{\mathrm{T}}\omega} & -\mu\sigma^{\mathrm{T}}\dfrac{Qc}{\epsilon^{\mathrm{T}}\omega} & -i\mu q^{\mathrm{L}}\sigma^{\mathrm{L}} & i\mu q^{\mathrm{L}}\sigma^{\mathrm{L}} \\ 0 & 0 & -i\nu\epsilon^{B}[Q^2+(q^{\mathrm{L}})^2] & -i\nu\epsilon^{B}[Q^2+(q^{\mathrm{L}})^2] \end{bmatrix} , \tag{6}$$

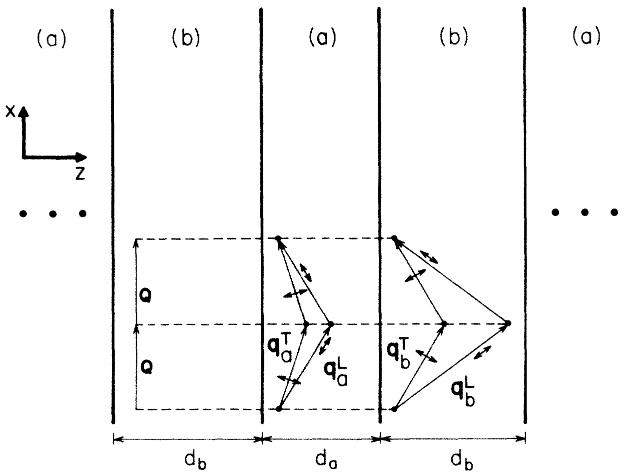

FIG. 1. Superlattice made up by alternating two conducting layers *a* and *b*. The wave vectors of the two transverse and the two longitudinal waves in each layer, and their common parallel projection are displayed. The coordinate system employed is also shown.

and

$$\sigma^{T}=(\epsilon^{T}-\epsilon^{B})\omega/4\pi i \;, \tag{7}$$

and

$$\sigma^{L}=(\epsilon^{L}-\epsilon^{B})\omega/4\pi i \tag{8}$$

are the transverse and longitudinal conduction-electron conductivities. Notice that $\epsilon^{L}=0$ in Eq. (8) since it is to be evaluated at the plasmon wave vector.

Since $B_{+}(z)$ and $B_{-}(z)$ are transverse, and $\phi_{+}(z)$ and $\phi_{-}(z)$ are longitudinal waves propagating along the Z direction with wave vectors q^{T}, $-q^{T}$, q^{L}, and $-q^{L}$ respectively, they are related at different points z and z' through

$$\begin{bmatrix} B_{+} \\ B_{-} \\ \phi_{+} \\ \phi_{-} \end{bmatrix}_{z} = \underline{T}(z-z') \begin{bmatrix} B_{+} \\ B_{-} \\ \phi_{+} \\ \phi_{-} \end{bmatrix}_{z'} \;, \tag{9}$$

where

$$\underline{T}(z-z')=\mathrm{diag}[e^{iq^{T}(z-z')},\ e^{-iq^{T}(z-z')},\ e^{iq^{L}(z-z')},\ e^{-iq^{L}(z-z')}] \;, \tag{10}$$

and diag($\cdots$) is a diagonal matrix constructor. Finally, Eqs. (5) and (9) lead to the 4×4 transfer matrix of one layer of width d,

$$\underline{M}_{l}=\underline{G}\,\underline{T}(d)\underline{G}^{-1} \;, \tag{11}$$

which relates the fields at its right boundary to those at its left boundary through

$$\begin{bmatrix} E_x \\ B_y \\ \mu j_z \\ 4\pi i \nu \rho \end{bmatrix}_{\mathrm{right}} = \underline{M}_{l} \begin{bmatrix} E_x \\ B_y \\ \mu j_z \\ 4\pi i \nu \rho \end{bmatrix}_{\mathrm{left}} \;. \tag{12}$$

The transfer matrix $\underline{M}_{l}$ can be written in blocks as

$$\underline{M}_{l}=\begin{bmatrix} \underline{M}_{l}^{TT} & \underline{M}_{l}^{TL} \\ \underline{M}_{l}^{LT} & \underline{M}_{l}^{LL} \end{bmatrix} , \tag{13}$$

where

$$\underline{M}_{l}^{TT}=\begin{bmatrix} C^{T} & i[(Z^{T})^{2}S^{T}-W^{T}W^{L}S^{L}] \\ iS^{T} & C^{T} \end{bmatrix} . \tag{14a}$$

$$\underline{M}_{l}^{TL}=iW^{L}\begin{bmatrix} S^{L} & i(C^{T}-C^{L}) \\ 0 & -S^{T} \end{bmatrix} , \tag{14b}$$

$$\underline{M}_{l}^{LT}=iW^{T}\begin{bmatrix} S^{T} & i(C^{L}-C^{T}) \\ 0 & -S^{L} \end{bmatrix} , \tag{14c}$$

and

$$\underline{M}_{l}^{LL}=\begin{bmatrix} C^{L} & i[(Z^{L})^{2}S^{L}-W^{L}W^{T}S^{T}] \\ iS^{L} & C^{L} \end{bmatrix} . \tag{14d}$$

Here we have introduced the following definitions:

$$Z^{T}=\frac{q^{T}c}{\epsilon^{T}\omega} \tag{15a}$$

is the surface impedance $Z^{T}\equiv E_{x}^{T}/B_{y}^{T}$ for a transverse plane wave traveling towards the right with wave vector q^{T}, and

$$Z^{L}=-\frac{\mu q^{L}\sigma^{L}}{\epsilon^{B}\nu[Q^{2}+(q^{L})^{2}]} \tag{15b}$$

is the corresponding surface impedance $Z^{L}\equiv\mu j_{z}^{L}/(4\pi i\nu\rho)$ for a longitudinal wave propagating with wave vector q^{L};

$$W^{T}=-\mu\sigma^{T}\frac{Qc}{\epsilon^{T}\omega} \tag{15c}$$

is the magnetic field–electric current response $W^{T}\equiv\mu j_{z}^{T}/B_{y}$ for a transverse wave, and

$$W^{L}=-\frac{Q}{\epsilon^{B}\nu[Q^{2}+(q^{L})^{2}]} \tag{15d}$$

is the corresponding density–electric field response $W^{L}\equiv E_{x}^{L}/(4\pi i\nu\rho)$ for a longitudinal wave; finally,

$$C^{T}\equiv\cos(q^{T}d) \;, \tag{15e}$$

$$C^{L}\equiv\cos(q^{L}d) \;, \tag{15f}$$

$$S^{T}\equiv\sin(q^{T}d)/Z^{T} \;, \tag{15g}$$

and

$$S^{L}\equiv\sin(q^{L}d)/Z^{L} \tag{15h}$$

contain the information about the layer's width. Our definitions (15a)–(15d) of the four impedance functions,

Z^{T}, Z^{L}, W^{T}, and W^{L}, are understandable if we regard B_y as the transverse response and ρ as the longitudinal response to the exciting fields E_x and j_z. We are not aware of previous attempts to define a longitudinal surface impedance Z^{L}, so we remark that it plays, for longitudinal waves, a role similar to that played by the usual transverse surface impedance Z^{T} in classical optics.[31] Furthermore, notice that the set of Eqs. (14) is invariant under the simultaneous interchange of the indices T and L on both their right- and left-hand sides.

Notice that since we chose continuous field quantities in Eq. (12), we need not worry anymore about the boundary conditions, and the transfer matrix for a multilayered system is simply given by the product of the transfer matrices of its constituents. However, the transfer matrices themselves depend on the choice of ABC's through the parameters μ and ν as shown by Eqs. (13)–(15).

B. Bulk normal modes of a periodic superlattice

In order to calculate the dispersion relation of the bulk modes of the superlattice, we first calculate the transfer matrix $\underline{M}$ for a complete period. As discussed above, the latter can be written simply as

$$\underline{M}=\underline{M}_l^b\underline{M}_l^a\ , \tag{16}$$

where $\underline{M}_l^a$ and $\underline{M}_l^b$ are the transfer matrices of layers a and b respectively, and are obtained from Eqs. (1)–(15) simply by appending the indices a or b to all the layer-dependent quantities such as Z^{L}, Z^{T}, W^{L}, etc.

The periodicity of the superlattice implies that the normal modes of the system can be obtained as Bloch waves such that

$$\begin{bmatrix} E_x \\ B_y \\ \mu j_z \\ 4\pi i\nu\rho \end{bmatrix}_{z+d} = e^{ipd}\begin{bmatrix} E_x \\ B_y \\ \mu j_z \\ 4\pi i\nu\rho \end{bmatrix}_{z}\ , \tag{17}$$

where $d=d_a+d_b$ is the superlattice period and p is Bloch's wave vector. Therefore, the dispersion relation $p=p(\omega)$ of the bulk normal modes is given implicitly by

$$\det(\underline{M}-e^{ipd}\underline{1})=0\ , \tag{18}$$

that is, e^{ipd} should be an eigenvalue of $\underline{M}$. We write the characteristic polynormal in $\Lambda=e^{ipd}$, $p(\Lambda)=\det(\underline{M}-\Lambda\mathbf{1})$, as

$$P(\Lambda)=\Lambda^2(\Lambda^2+\alpha_3\Lambda+\alpha_2+\alpha_1/\Lambda+\alpha_0/\Lambda^2)\ . \tag{19}$$

Now we remark that if p is a solution of Eq. (18) representing, for instance, a Bloch wave traveling towards the right, then $-p$ is also a solution and it represents the same wave but traveling towards the left. Therefore, if Λ is a zero of $P(\Lambda)$, so is $1/\Lambda$.[32] From Eq. (19) we see that we should have $\alpha_0=1$ and $\alpha_1=\alpha_3$, and therefore the fourth-order equation in e^{ipd}, Eq. (18), can be written simply as

$$4\cos^2(pd)+2\alpha_3\cos(pd)+\alpha_2-2=0\ , \tag{20}$$

which is only quadratic in $\cos(pd)$ and can be solved analytically for p in terms of the coefficients

$$\alpha_3=-\mathrm{Tr}(\underline{M}) \tag{21a}$$

and

$$\alpha_2=[\mathrm{Tr}(\underline{M})^2-\mathrm{Tr}(\underline{M}^2)]/2\ . \tag{21b}$$

After substituting Eqs. (13)–(15) in Eqs. (16) and (21), and performing a quite tedious algebra in order to condense the resulting $\sim 10^2$ terms, we obtain

$$\alpha_3=-2(\mathrm{L}+\mathrm{T})+K(S_a^{\mathrm{L}}S_b^{\mathrm{T}}+S_a^{\mathrm{T}}S_b^{\mathrm{L}}) \tag{22a}$$

and

$$\begin{aligned}\alpha_2=2+4\mathrm{LT}+K^2S_a^{\mathrm{T}}S_a^{\mathrm{L}}S_b^{\mathrm{T}}S_b^{\mathrm{L}}\\ -2K[(C_a^{\mathrm{T}}S_b^{\mathrm{T}}+S_a^{\mathrm{T}}C_b^{\mathrm{T}})(C_a^{\mathrm{L}}S_b^{\mathrm{L}}+S_a^{\mathrm{L}}C_b^{\mathrm{L}})\\ -(S_a^{\mathrm{T}}S_a^{\mathrm{L}}+S_b^{\mathrm{T}}S_b^{\mathrm{L}})]\ ,\end{aligned} \tag{22b}$$

where

$$T=C_a^{\mathrm{T}}C_b^{\mathrm{T}}-[(Z_a^{\mathrm{T}})^2+(Z_b^{\mathrm{T}})^2]S_a^{\mathrm{T}}S_b^{\mathrm{T}}/2\ , \tag{23a}$$

$$L=C_a^{\mathrm{L}}C_b^{\mathrm{L}}-[(Z_a^{\mathrm{L}})^2+(Z_b^{\mathrm{L}})^2]S_a^{\mathrm{L}}S_b^{\mathrm{L}}/2\ , \tag{23b}$$

and

$$K=(W_a^{\mathrm{T}}-W_b^{\mathrm{T}})(W_a^{\mathrm{L}}-W_b^{\mathrm{L}})\ . \tag{23c}$$

We remark that in the absence of spatial dispersion, the normal modes of the system are given by pure transverse waves in each layer, coupled at their interfaces by the electromagnetic boundary conditions. These modes obey the dispersion relation $\cos(pd)=T$.[20] In a similar fashion, $\cos(pd)=\mathrm{L}$ is the dispersion relation of normal modes made up of pure longitudinal waves[33] coupled at the interfaces in order to obey the additional boundary conditions. In the limit $K\to 0$, Eq. (20) factors as $4[\cos(pd)-T][\cos(pd)-L]=0$, so that each one of the two normal modes discussed above propagates unaffected by the presence of the other. Thus we may regard K as a measure of the coupling between transverse and longitudinal modes. Notice that K is proportional to Q^2 and that it vanishes for propagation along the superlattice. We also point out that for any value of K, Eq. (20) has two pairs $\pm p$ of solutions which evolve continuously from the pure transverse and the pure longitudinal modes at $K=0$. This solution survives even in the nonretarded regime, attained simply by replacing q_a^{T} and q_b^{T} with iQ in Eqs. (15). Thus we have twice as many solutions than found by previous workers.[14,15,22] The relative importance of the two sets of modes, and the possibility of neglecting one of them[22] in different situations, is an important question which will be addressed in the future.

Other limiting situations can be easily explored. The local limit of the dispersion relations is obtained by letting the imaginary part of q_a^{L} and q_b^{L} go to infinity,[21] so that the charge density gets confined to the interfaces. In this case, transverse and longitudinal modes also become uncoupled, although the latter's wave vector diverges and we are left only with the same dispersion relation as obtained by classical optics. The limiting case of a local-nonlocal superlattice should be investigated with some care, as it can be attained in two nonequivalent ways.[34] We can either let $\omega_p^b \to 0$ and $\beta_b \to 0$ in order to obtain a conductor-insulator superlattice, or we can neglect the stiffness β_b while retaining a finite value for ω_p^b in order to get a local-nonlocal conductor superlattice. Both of these cases have been studied before[20–22] using a specific ABC. A rich spectrum of normal modes, consisting of guided bulk plasmons, surface plasmons, guided and/or extended transverse waves, all coupled among themselves, was found. Here we remark that similar results are obtained at the conductor-insulator limit when we use the ABC's referred to above as models I and III, and also at the local-nonlocal conductor limit when we use model III. However, in the remaining situations, there is no transverse longitudinal coupling,[35] i.e., the normal modes of the local-nonlocal superlattice behave as though no plasma waves were present in the spatially dispersive layers.

III. RESULTS

In the present section, we use Eqs. (20)–(23) in order to calculate the dispersion relation of the electromagnetic normal modes of highly doped semiconductor superlattices. The results for metallic superlattices are qualitatively similar. In order to compare our results with previous works, we choose the same parameters as in Refs. 22 and 14: the widths of the layers are taken to be $d_a = 100$ Å and $d_b = 5d_a$, the free-carrier densities $n_a = 2.33\times10^{17}$ cm^{-3} and $n_b = 2n_a$, we ignore the contribution of the bound electrons to the response, $\epsilon^B = 1$, and we assume a very large electronic relaxation time $\tau = 10^4/\omega_p^a$. The plasma frequencies and stiffness constants are obtained from

$$(\omega_p^\alpha)^2 = 4\pi n_\alpha e^2/m \text{ and } \beta_\alpha^2 = \frac{3\hbar^2}{5m^2}(3\pi^2 n_\alpha)^{2/3},$$

where e and m are the electronic charge and mass, respectively, and the index α can take the values a or b.

Since Eq. (20) is quadratic in $\cos(pd)$, there are two solutions for each frequency. These were sorted out according to the imaginary part of the Bloch's wave vector p. In Fig. 2 we show the real and the imaginary parts of the dispersion relation $p = p' + ip''$ versus ω of the solution with the smallest imaginary part, obtained for a fixed value of $Q = 0.5/d_a$ and using the ABC's we referred to before as model III. Several kinds of modes can be identified in this figure.

First, there are modes corresponding to surface plasmons (SP's) propagating along each conductor-conductor interface. The nonzero overlap of their electric field at each layer gives origin to two bulk bands. These two SP-SP bands have been discussed before for local-local and local-nonlocal conducting superlattices.[9,10,22] It is interesting to note that they are modified slightly by spatial dispersion.

Next, there are bands corresponding to guided plasmons (GP's) in the low-density layers—in this case, the a layers—coupled among themselves by the evanescent mostly transverse (ET) waves they induce in the

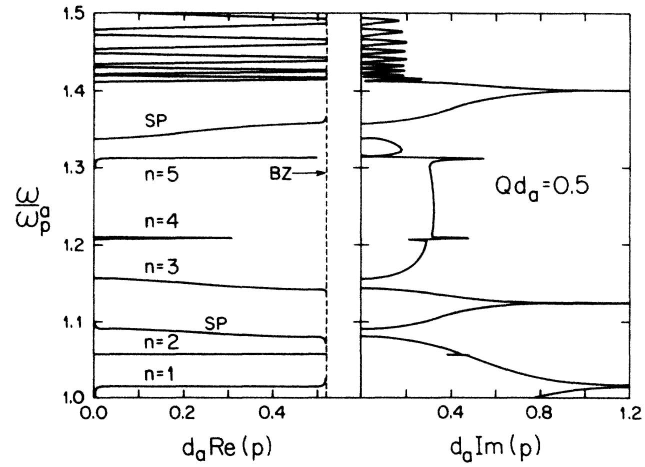

FIG. 2. Dispersion relation $p = p' + p''$ vs ω of the small p'' modes obtained within model III for a superlattice made up of two alternating conductors a and b with $d_a = 100$ Å, $d_b = 5d_a$, $n_a = 2.33\times10^{17}$, $n_b = 2n_a$, $\epsilon^B = 1$, and $\tau = 10^4/\omega_p^a$. The parallel wave vector is taken to be $Q = 0.5/d_a \gg \omega/c$, so retardation effects are unimportant. The results were obtained using model III. The SP-SP modes, the index n of the GP-ET modes, and the boundary of the Brillouin zone (BZ) are indicated.

high-density b layers. Their frequencies lie around the single-film longitudinal resonance frequencies ω_n given by

$$\omega_n^2 = (\omega_p^a)^2 + \beta_a^2[Q^2 + (n\pi/d_a)^2], \quad n = 1, 2, \ldots, \tag{24}$$

but they are shifted towards lower frequencies. The origin of this shift is the finite decay length of longitudinal waves in the b layers, which leads to some plasmon spillover from a layers. Since the decay length increases with ω_n, so does the frequency shift. Notice that the modes labeled with even n have a shorter bandwidth than those with odd n, since their corresponding plasmons produce a smaller field in the b layers. For the same reason, the imaginary part of their wave vector is larger.

Finally, above $\omega_p^b \approx 1.4\omega_p^a$ bulk propagating plasmons (PP's) exist in both kinds of layers, giving rise to an almost longitudinal PP-PP mode whose dispersion relation has a series of gaps at the center and the edges of the Brillouin zone due to the periodicity of the system.[15]

Comparing Fig. 2 with Fig. 1 of Ref. 22, we find the same SP-SP and similar GP-ET bands. However, the latter appear shifted since in Ref. 22 the b layers were assumed local and therefore the effects of plasmon spillover were excluded. The position and widths of the bands we obtained also correspond closely to those shown in Figs. 1 and 2 of Ref. 14, since retardation is unimportant given the large value of Q we have chosen. Although the mode $n = 1$ is missing from the results of Ref. 14, our Fig. 2 shows that it has a small decay distance $1/p''$ so it is of small account. A mode similar to the almost longitudinal PP-PP mode above ω_p^b has been obtained recently[15] by neglecting completely all transverse fields.

In Fig. 3 we show the dispersion relation p versus ω of the second solution of Eq. (20), that with the larger p'',

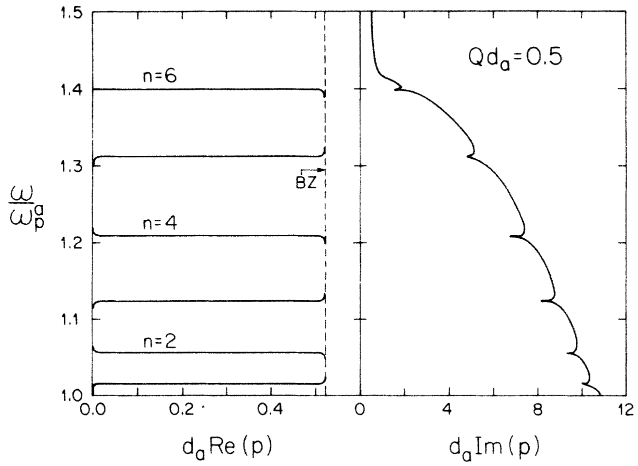

FIG. 3. Dispersion relation p vs ω of the large p'' modes corresponding to the same parameters as in Fig. 2. The index n of the GP-EP modes is indicated.

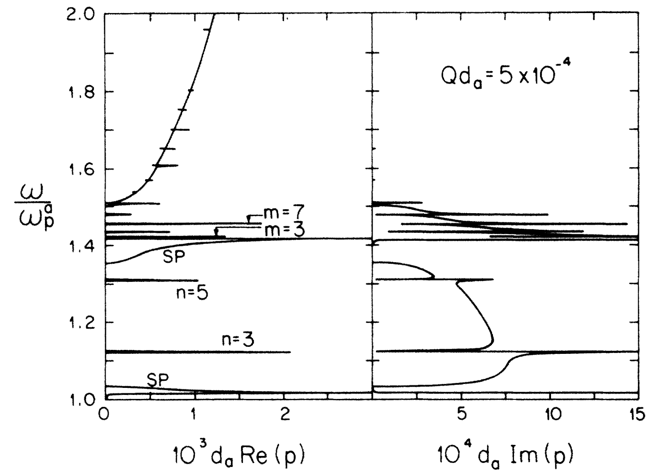

FIG. 4. Dispersion relation p vs ω of the small p'' modes for a small parallel wave vector $Q=5\times10^{-4}/d_a\sim\omega/c$, so that retardation effects are important. All other parameters are as in Fig. 2. The index m of some PT-GP modes is also indicated.

using the same parameters as in Fig. 2. A series of extremely narrow bands can be seen around the longitudinal resonance frequencies ω_n. Therefore there are two bulk modes, those shown in Fig. 2 and those in Fig. 3, corresponding to each guided plasmon in the a layers. The reason for this multiplicity is that below ω_p^b there are two mechanisms coupling adjacent a layers: the evanescent transverse (ET) waves and the evanescent plasmons (EP) in the b layers. Since the latter have a much smaller decay length than the former, they generate a smaller coupling and hence they produce the flatter GF-EP bands. These modes are absent from Ref. 22 where the evanescent longitudinal waves at the b layers were neglected. Neither were they reported in Ref. 14. However, they correspond to the low-frequency modes obtained in Ref. 15.

In order to investigate the effects of retardation, in Fig. 4 we have plotted the dispersion relation of the long-decay-length modes of the same superlattice as in Figs. 2 and 3, but for a small parallel wave vector $Q=5\times10^{-4}/d_a$. At frequencies below ω_p^b we find again two SP-SP and the odd-numbered GP-ET modes. The even-numbered ones cannot be seen in this figure since the weak GP-ET coupling is further reduced when Q is decreased. Between ω_p^b and the critical frequency $\omega_c=[(\omega_p^b)^2+(Qc)^2]^{1/2}\approx1.51\omega_p^a$, longitudinal waves can propagate in the b layers but transverse waves cannot. Therefore, we find a series of modes (PT-GP) consisting of odd-numbered guided plasmons in the b layers coupled by the almost constant propagating transverse (PT) waves in the a layers, with frequencies very close to

$$\omega_m'=\{(\omega_p^b)^2+\beta_b^2[Q^2+(m\pi/d_b)^2]\}^{1/2} . \qquad (25)$$

Finally, above the critical frequency both kinds of layers become transparent to longitudinal and transverse waves. The dispersion relation shown in Fig. 4 follows closely that of transverse waves (PT-PT) in a local superlattice, but with sharp structures due to longitudinal resonances.

In Fig. 5 we show the short-decay-length modes corresponding to the same parameters as in Fig. 4. Below ω_p^b we find GP-EP modes similar to those shown in Fig. 3. Above ω_p^b we obtain the mostly longitudinal PP-PP mode that appeared previously in Fig. 2. Notice that Q is so large in Figs. 2 and 3 that a propagating PT-PT mode cannot exist, so its decay length is much smaller than that of the PL-PL mode. This situation is reversed in Figs. 4 and 5.

We also investigated how our results are modified by different choices of ABC. To that effect, we repeated the calculations above but using models I and II instead of model III. The results for model II corresponding to those in Figs. 4 and 5 are shown in Figs. 6 and 7, respectively. Notice that the SP-SP bands displayed in Fig. 6 are almost indistinguishable from those present in Fig. 4

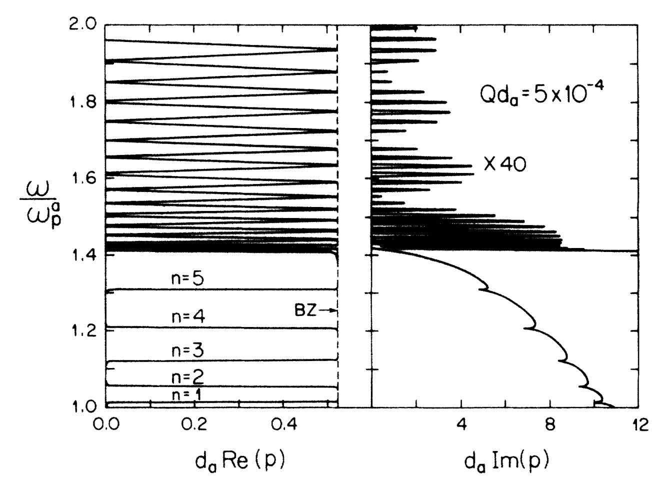

FIG. 5. Dispersion relation p vs ω of the large p'' modes for $Q=5\times10^{-4}/d_a$. All other parameters are as in Fig. 2.

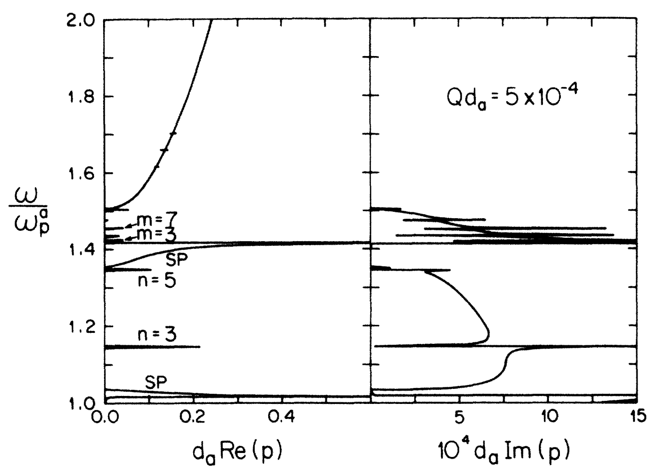

FIG. 6. Dispersion relation p vs ω of the small p'' modes calculated within model II. All other parameters are as in Fig. 4.

since they are almost unaffected by spatial dispersion and therefore they are not influenced by the ABC's. On the other hand, the GP-ET bands are noticeably shifted to higher frequencies since, in model II, the plasmon spillover is considerably diminished. The $n=5$ mode almost overlaps the upper SP-SP band, and it actually does when Q increases. Between ω_p^a and ω_c we find PT-GP propagation at the same frequencies in both figures, but the bands in Fig. 6 are narrower due to a decreased L-T coupling. Recall that this coupling vanishes in model II in the limit when one of the conductors becomes local. In fact this coupling is so weak that the plasmon-originated structure in the PT-PT mode above ω_c all but disappears. The GP-EP bands appearing in Fig. 7 are displaced towards higher frequencies, such as those in Fig. 6, while the PP-PP mode above ω_p^b closely resembles that in Fig. 5, except for the distribution of gap widths and the heights of the peaks of p''.

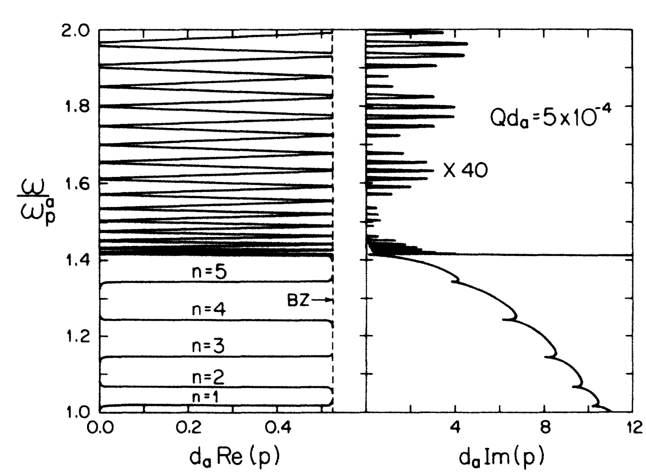

FIG. 7. Dispersion relation p vs ω of the large p'' modes calculated within model II. All other parameters are as in Fig. 2.

The results obtained within model I differ much less from model III than those of model II, and so they are not shown. The reason for this is that whereas μ and ν are constants in model III, in model I μ is constant and ν is proportional to $n^{-1/3}$ and therefore it has a small variation of only about 25% between consecutive layers. On the other hand, μ and ν change in model II by 60% and 100%, respectively, in going from one layer to the next. The main differences we found in model I consist of a small decrease in the frequency of the guided plasmon modes and a diminished coupling between the even-numbered and transverse waves.

IV. CONCLUSIONS

In this paper we have developed a transfer-matrix formalism in order to study within hydrodynamic models the optics of spatially dispersive conducting layered media, taking into account the coupling between p-polarized transverse waves and longitudinal waves at each interface.

In order to allow for the presence of longitudinal waves, we have introduced 4×4 transfer matrices instead of the usual 2×2 matrices that appear in classical optics.[17] They are not unlike the 4×4 matrices that show up in elasticity theory.[18] In order to make our formalism suitable for different models of the conductor-conductor interface, we expressed the transfer matrix in terms of the two parameters μ and ν that define the set of additional boundary conditions chosen. Thus we can turn from one hydrodynamic model to another simply by adjusting μ and ν without modifying our formulas.

We applied the transfer-matrix formalism to the calculation of the bulk electromagnetic normal modes of an infinite periodic superlattice made up of two alternating homogeneous conductors. A quadratic equation for $\cos(pd)$ was found from which two sets, p and $-p$, of Bloch's wave vectors can be obtained analytically for each frequency ω and each value of the parallel wave vector Q. We remark that besides the period d of the superlattice, there are two very dissimilar length scales in our problem: the decay length (or the wavelength) of transverse and longitudinal waves. Since the transfer matrices have terms which are exponential functions of these distances, they are highly unbalanced, and a straightforward numerical calculation of the dispersion relation is bound to fail due to numerical instabilities and accumulation of rounding errors. Thus it is advantageous to have analytical results available. They also permitted us to explore several limiting cases, such as the uncoupling of transverse and longitudinal waves, the conductor-insulator superlattice, and the local-nonlocal conducting superlattice.

The reason we obtained two modes at each ω and Q can be easily understood by first considering the limit in which both conductors are identical. In this case the superlattice becomes homogeneous and it has two kinds of normal modes which are the usual transverse and longitudinal waves. However, their dispersion relation is folded back at the Brillouin-zone boundary $p=\pi/d$ due to the artificial periodicity d. Now, as we allow the two conductors to become different, the periodicity d acquires a physical meaning, gaps open at the Brillouin-zone center and boundary, and the modes couple among themselves whenever their dispersion relations approach each other, but the existence of two sets of solutions remains.

We have identified a very rich spectrum of normal modes for the superlattice. First, we found two bands (SP-SP) corresponding to surface plasmons propagating along each interface and coupled together through the tails of their evanescent fields. These bands also appear in local systems and they are slightly modified by spatial dispersion. Then there are modes made up of guided plasmons in the low-density layers, that is, propagating longitudinal waves reflected back and forth at the boundaries of the a layers such that their wavelength fits approximately a half-integer number of times in layer's width. The guided plasmons of neighbor a layers interact either through the longitudinal or through the transverse evanescent fields they induce in the high-density b layers, thus giving origin to two kinds of bulk modes, GP-ET and GP-EP. At higher frequencies we detected bands made up of resonant guided plasmons in the b layers coupled together through propagating transverse waves at the a layers (PT-GP). Finally, we found modes mainly made up from either transverse or longitudinal waves propagating in both kinds of layers (PT-PT and PP-PP). Modes coming from guided transverse waves were not obtained since the layers we considered were too thin.

Our formalism can be used in the retarded and the nonretarded regions. We have found a richer spectrum in the retarded region due to the possibility of transverse wave propagation. We have also explored the differences between several models of conductor interfaces. The main discrepancies obtained were in the frequencies of the guided plasmon modes due to the differences in plasmon spillover, and in the bandwidth of those modes involving both transverse and longitudinal waves due to differences in their coupling strength. The possible observation of the multitude of modes we obtained through their interaction with external probes, such as incident light or charged particles, will be the object of future research. More realistic models of conducting superlattices, taking into account electron-hole excitations, quantum electronic interference effects at surfaces, and size effects,[36] should also be investigated.

ACKNOWLEDGMENTS

We want to acknowledge fruitful discussions with R. G. Barrera and the technical assistance of J. Hernandez. We are also grateful for the hospitality of Laboratorio de Cuernavaca, Instituto de Física, Universidad Nacional Autónoma de México. This work was supported by Consejo Nacional de Ciencia y Tecnología (CONACyT), Mexico, under Grant No. PCEXCNA-040428.

[1]Proceedings of the International Conference on Electron Properties of 2D Systems, New London, New Hampshire, edited by Frank Stern [Surf. Sci. **113**, (1982)].

[2]A. L. Fetter, Ann. Phys. (N.Y.) **81**, 367 (1973); **88**, 1 (1978); S. Das Sarma and J. J. Quinn, Phys. Rev. B **25**, 7603 (1982).

[3]G. F. Giuliani and J. J. Quinn, Phys. Rev. Lett. **51**, 919 (1983); G. Qin, G. F. Giuliani, and J. J. Quinn, Phys. Rev. B **28**, 6144 (1983); G. F. Giuliani, G. Qin, and J. J. Quinn, Surf. Sci. **142**, 433 (1984); J. K. Jaim and P. B. Allen, Phys. Rev. Lett. **54**, 947 (1985); R. A. Mayanovic, G. F. Giuliani, and J. J. Quinn, Phys. Rev. B **34**, 5309 (1986).

[4]S. Das Sarma, Akiko Koboyashi, and R. E. Prange, Phys. Rev. Lett. **56**, 1280 (1986); Phys. Rev. B **34**, 5309 (1986).

[5]Pavel Hawrylak and John J. Quinn, Phys. Rev. Lett. **57**, 380 (1986).

[6]A. C. Tselis, G. González de la Cruz, and J. J. Quinn, Solid State Commun. **46**, 779 (1983); A. C. Tselis and J. J. Quinn, Phys. Rev. B **29**, 3318 (1984); Pawel Hawrylak, Gunnar Eliasson, and John J. Quinn, *ibid.* **34**, 5368 (1986); R. D. King and J. C. Inkson, J. Phys. C **19**, L15 (1986).

[7]H. Köstin, R. Jost, and W. Lems, Phys. Status Solidi A **29**, 87 (1975); I. Hanberg, C. G. Granqvist, K. F. Berggren, B. E. Sernelius, and L. Ergströn, Vacuum **35**, 207 (1985); F. Demichelis, E. Minetti-Mezzeti, V. Smurro, A. Tagliaferro, and E. Tresso, J. Phys. D **18**, 1825 (1985).

[8]Z. A. Zheng, C. M. Falco, and J. B. Ketterson, Appl. Phys. Lett. **38**, 424 (1981); I. K. Schuller and C. M. Falco, Surf. Sci. **113**, 443 (1982); R. Vaglo, A. Cucolo, and C. M. Falco, J. Phys. (Paris) Colloq. **45**, C5-499 (1984).

[9]R. E. Camley and D. L. Mills, Phys. Rev. B **29**, 1695 (1984); G. F. Giuliani, J. J. Quinn, and R. F. Wallis, J. Phys. (Paris) Colloq. **45**, C5-285 (1984).

[10]R. Szenics, R. F. Wallis, G. F. Giuliani, and J. J. Quinn, Surf. Sci. **166**, 45 (1986).

[11]V. M. Agranovich and V. E. Kravstov, Solid State Commun. **55**, 85 (1985); P. Apell, O. Hunderi, and R. Monreal, Phys. Scr. **34**, 348 (1986).

[12]Martin Klein, Rubén G. Barrera, and W. Luis Mochán (unpublished).

[13]W. Luis Mochán, R. Fuchs, and Rubén G. Barrera, Phys. Rev. B **27**, 771 (1983); P. J. Feibelman, Prog. Surf. Sci. **12**, 287 (1982).

[14]G. Eliasson, G. F. Giuliani, and J. J. Quinn, Phys. Rev. B **33**, 1405 (1986).

[15]M. Babiker, J. Phys. C **19**, L773 (1986).

[16]G. González de la Cruz and J. J. Quinn (unpublished); G. González de la Cruz, G. Eliasson, and J. J. Quinn, in *Proceedings of the International Workshop on Electrodynamics of Interfaces and Composite Systems, Taxco, México, 1987,* edited by R. G. Barrera and W. L. Mochán (World-Scientific, Singapore, in press).

[17]E. Hecht and A. Zajac, *Optics* (Addison-Wesley, Reading, Mass., 1974), Sec. 9.9.

[18]B. L. N. Kennet, *Seismic Wave Propagation in Stratified Media* (Cambridge University Press, Cambridge, England, 1985), Sec. 2.2.

[19]P. A. Mello, Phys. Rev. B **35**, 1082 (1987); P. A. Mello, P. Pereyra, and N. Kumar, Ann. Phys. (N.Y.) (to be published).

[20]W. Luis Mochán, Marcelo del Castillo-Mussot, and Rubén G. Barrera, Phys. Rev. B **35**, 1088 (1987).

[21]Marcelo del Castillo-Mussot, W. Luis Mochán, and Rubén G. Barrera, in *Lectures in Surface Science,* Proceedings of the

Fourth Latin-American Symposium on Surface Science, Caracas, Venezuela, 1986, edited by Germán R. Castro and Manuel Cardona (Springer, Berlin, 1987), p. 28.

[22]Marcelo del Castillo-Mussot and W. Luis Mochán, Phys. Rev. B **36**, 1779 (1987).

[23]F. Forstmann, Z. Phys. **32**, 385 (1975).

[24]C. Schwartz and W. L. Schaich, Phys. Rev. B **26**, 7008 (1982).

[25]P. Ahlqvist and P. Apell, Phys. Scr. **25**, 587 (1982).

[26]J. D. Jackson, *Classical Electrodynamics* (Wiley, New York, 1975), Sec. I.5.

[27]D. L. Johnson and P. R. Rimbey, Phys. Rev. B **4**, 2398 (1976); P. Halevi and G. Hernandez-Cocoletzi, Phys. Rev. Lett. **48**, 1500 (1982).

[28]F. Forstmann and H. Stenschke, Phys. Rev. Lett. **38**, 1365 (1977); Phys. Rev. B **17**, 1489 (1978).

[29]A. D. Boardman and R. Ruppin, Surf. Sci. **112**, 153 (1981).

[30]G. Eliasson, G. F. Giuliani, and J. J. Quinn, Phys. Rev. B **31**, 6534 (1985).

[31]L. D. Landau and M. M. Lifshitz, *Electrodynamics of Continuous Media* (Pergamon, New York, 1960), p. 280.

[32]In our case, this can be seen from the reflection symmetry of the system. However, it is not a general property of the 4×4 matrices of layered conducting systems, unless certain conditions are obeyed by the set of ABC's imposed. This point will be further discussed elsewhere.

[33]This dispersion relation was obtained in Ref. 15 within model II, where the potential in each layer was written as a superposition of two longitudinal waves which solve the hydrodynamic equation of motion. However, the two transverse or the two waves which solve Laplace's equation in the nonretarded regime, and which are required at each layer in order to satisfy the electromagnetic boundary conditions, were overlooked.

[34]Marcelo del Castillo-Mussot and W. Luis Mochán, Solid State Commun. **62**, 555 (1987).

[35]A. P. Boardman and M. R. Parker, Phys. Status Solidi B **71**, 329 (1975).

[36]P. Apell, Phys. Scr. **32**, 408 (1985).